Ring Current Enhanced Vibrational Circular Dichroism in the CH-Stretching Motions of Sugars

M. Germana Paterlini, Teresa B. Freedman,* and Laurence A. Nafie*

Contribution from the Department of Chemistry, Syracuse University, Syracuse, New York 13244. Received August 16, 1985

Abstract: The vibrational circular dichroism (VCD) in the CH-stretching spectra of several pyranose sugars is interpreted in terms of the vibrational ring current mechanism. The large monosignate negative VCD in D-mannose, D-gulose, and D-glucose-2-d_1 in D_2O solution is attributed to an oscillating magnetic moment produced by vibrationally generated currents in intramolecularly hydrogen-bonded rings involving carbons 2, 3, and 4. These current contributions cancel in D-glucose, and the VCD intensity is greatly diminished. In L-sorbose and D-xylose, nearly mirror image monosignate VCD spectra result from currents around the pyranose ring, generated by the C(5) methylene hydrogen-stretching modes. The analysis of the VCD spectra demonstrates that the vibrational ring current mechanism is responsible for virtually all the observed VCD features in the CH-stretching region of carbohydrates in aqueous solution.

I. Introduction

Vibrational circular dichroism (VCD)[1-4] has been found to be sensitive to intramolecular association in chiral molecules in solution, as a result of the vibrational ring current intensity mechanism.[4-8] The concept of vibrationally generated ring currents in molecules was originally proposed to explain the observed VCD bias in the CH-stretching region of the amino acids, amino acid transition-metal complexes, and α-hydroxy acids. The bias was attributed to the methine CH-stretching vibration which exhibits enhanced VCD intensity. According to the proposed mechanism, the methine-stretching motion in amino acids generates an oscillating electronic current around the intramolecular ring closed by a hydrogen bond between the amine and carboxylate functional groups. More recently, vibrational ring currents have been shown to provide an explanation for the VCD in wider classes of molecules, intramolecular association, and vibrational modes.[4,7,8] It now appears that vibrationally generated ring currents represent a fundamentally new mechanism of VCD intensity, associated quite often with large VCD intensity. Two empirical rules have been formulated that are consistent with VCD spectra available to date, which govern the direction of current flow around a ring for a given phase of driving nuclear motion (momentum).[7] A theoretical basis for describing vibrational ring currents has been formulated.[9] The present work on sugars further demonstrates the capability of the ring current intensity mechanism to explain observed VCD features. For the sugars in the CH-stretching region, virtually all the VCD effects can be attributed to this mechanism.

The sugars form an important class of molecules for testing the ring current mechanism of VCD, since a wide variety of sugars are available which vary in configuration at the chiral centers and therefore vary in the extent and geometry of the intramolecular hydrogen-bonding interactions that form rings. In addition, the presence of a heteroatom within the nonplanar, covalent ring allows vibrationally generated ring current effects to be investigated for the first time in this class of molecular ring.

VCD spectra of sugars in both the CH and mid-infrared regions have been previously reported. The CH-stretching VCD spectra

of α- and β-methyl D-glucoside in D_2O solution[10] were observed to have an approximate mirror image relationship, and deuteration of the methyl group caused substantial reduction in the VCD. Since α- and β-methyl D-glucosides differ in absolute configuration at the anomeric carbon atom but not at the remaining chiral centers, the CH-stretching VCD in these two molecules was attributed primarily to the methyl group vibrations.

Havel[11] has surveyed the CH-stretching VCD of eight aldohexoses and a number of other pyranose sugars including 6-deoxyaldohexoses, aldopentoses, and 2-ketohexoses in D_2O solution. The VCD spectra of these sugars consist of either very weak signals or strong, broad monosignate bands. A correlation was found between the chiral arrangement of the C(2)H, C(3)H, and C(4)H bonds and the presence (or absence) and sign of the VCD, but the relative magnitudes of the VCD for different sugars and the origin of the correlation could not be explained. The CH-stretching VCD spectra of aldohexose peracetates in dilute CCl_4 solutions were also reported.[11] The VCD and absorption spectra in the peracetates were considerably more structured, including bisignate VCD features. An overall net negative VCD bias was observed in the CH-stretching region for the aldohexose peracetates, which cannot arise due to nuclear coupling effects alone.

A more recent mid-infrared FTIR–VCD study on sugars dissolved in Me_2SO-d_6[12] has identified a band near 1150 cm^{-1} for which a correlation is found between the sign of the VCD and the chiral arrangement of axial and equatorial C–O and C–C bonds to ring –OH or –CH$_2$OH substituents.

As a basis for interpreting these earlier investigations on sugars in light of more recently recognized contributions to VCD from vibrationally generated ring currents, we have recorded the VCD in the CH-stretching region for selected pyranose sugars which are predicted to have a range of ring current contributions. The VCD spectra of three specifically deuterated isotopomers of glucose have also been recorded in order to clarify assignments and determine the contributions from the C(6)H$_2$, C(2)H, and C(1)H vibrations.

II. Experimental Section

L-Sorbose and the D and L enantiomers of glucose, mannose, gulose, and xylose were purchased from Sigma. The isotopes D-glucose-1-d_1 and D-glucose-6,6-d_2 were obtained from MSD Isotopes. D-Glucose-2-d_1 was a gift from A.S. Perlin (McGill University). All samples were exchanged twice with D_2O. Spectra were obtained by using a variable path length BaF_2 cell, at 1.0 M concentration in D_2O and 0.11 mm path length with the exception of D-glucose-1-d_1 (0.5 M; 0.15 mm) and D-glucose-2-d_1 (~0.9 M; 0.05 mm). Due to the small amount of the isotopic samples available, the concentrations for these species are less certain. In the case

(1) Keiderling, T. A. *Appl. Spectrosc. Rev.* **1981**, *17*, 189.
(2) Nafie, L. A. In "Advances in Infrared and Raman Spectroscopy"; Clark, R. J. M., Hester, R. E., Eds.; Wiley-Heyden: London, 1984; Vol. 11, p 49.
(3) Stephens, P. J.; Lowe, M. A. *Annu. Rev. Phys. Chem.* **1985**, *36*, 213.
(4) Freedman, T. B.; Nafie, L. A. In "Topics in Stereochemistry"; Eliel, E., Wilen, S., Allinger, N., Eds.; Wiley: New York, 1986; Vol. 17, in press.
(5) Nafie, L. A.; Oboodi, M. R.; Freedman, T. B. *J. Am. Chem. Soc.* **1983**, *105*, 7449.
(6) Oboodi, M. R.; Lal, B. B.; Young, D. A.; Freedman, T. B.; Nafie, L. A. *J. Am. Chem. Soc.* **1985**, *107*, 1547.
(7) Freedman, T. B.; Balukjian, G. A.; Nafie, L. A. *J. Am. Chem. Soc.* **1985**, *107*, 6213.
(8) Young, D. A.; Lipp, E. D.; Nafie, L. A. *J. Am. Chem. Soc.* **1985**, *107*, 6205.
(9) Nafie, L. A.; Freedman, T. B. *J. Phys. Chem.* **1986**, in press.

(10) Marcott, C.; Havel, H. A.; Overend, J.; Moscowitz, A. *J. Am. Chem. Soc.* **1978**, *100*, 7088.
(11) Havel, H. A. Ph.D. Thesis, University of Minnesota, Minneapolis, 1981.
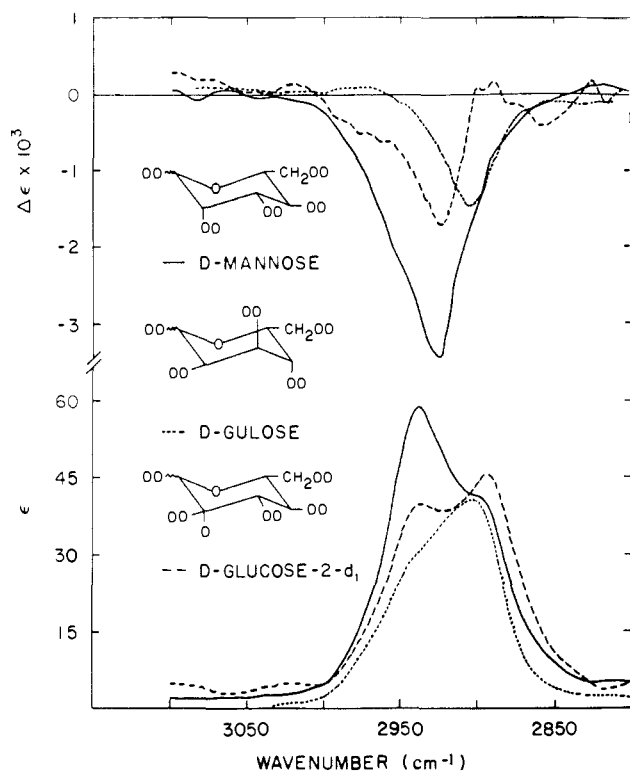(12) Back, D. M.; Polavarapu, P. L. *Carbohydr. Res.* **1984**, *133*, 163.

Figure 1. VCD and absorbance spectra in the CH-stretching region of D-mannose and D-gulose; 1.0 M in D_2O 0.11-mm path length, and D-glucose-2-*d*, ~0.9 M in D_2O, 0.05-mm path length.

of D-glucose-2-d_1, the molar absorptivity, ϵ, was normalized to that of D-glucose at 2892 cm^{-1}, where only minor contribution from the C(2)H stretch is expected. Spectra of D-mannose were also obtained at 0.2 M concentration.

VCD spectra were recorded on a dispersive grating instrument previously described,[13] at 10-s time constant and 12–14-cm^{-1} spectral resolution. The spectra shown here of L-sorbose, D-xylose, and D-gulose are the average of eight scans collected by using an IBM 9000 computer. The remaining spectra are redrawn from single scans on a chart recorder. Absorption spectra were obtained on a Nicolet 7199 FTIR at 4-cm^{-1} resolution. The VCD spectra have been corrected for base-line and absorption artifacts which were removed by comparing the VCD of the L and D enantiomers when both were available. The glucose base line was used for D-glucose-l-d_1 and D-glucose-6,6-d_2, the D_2O base line for D-glucose-2-d_1, and the xylose base line for L-sorbose. The noise level in the instrument was such that we have confidence in VCD features for which $\Delta\epsilon/\epsilon > 10^{-5}$.

Spectral simulations were obtained by using the Nicolet curve analysis program.

III. Results

The absorption and VCD spectra in the 2800–3050-cm^{-1} region for D_2O solutions of D-mannose, D-gulose, and D-glucose-2-d_1 are compared in Figure 1, the spectra of D-glucose and three deuterated D-glucose isotopomers in Figure 2, and the spectra of D-xylose, L-sorbose, and D-glucose in Figure 3, for the same $\epsilon(10^3$ cm^2 mol^{-1}) and 10^3 $\Delta\epsilon$ (10^3 cm^2 mol^{-1}) scales. Peak frequencies and intensities are compiled in Table I. The anisotropy ratio measured at 2925 cm^{-1} for D-mannose in 0.2 M D_2O solution (the lowest concentration for which VCD could be reliably measured) was the same as that observed for the 1.0 M solution. Spectra in the C–D-stretching region, ~2200 cm^{-1}, could not be obtained in either D_2O or H_2O solution due to interference from solvent absorption.

The sugars included in this study exist as an equilibrium mixture of pyranose, furanose, and acyclic forms and of α- and β-anomeric

(13) (a) Diem, M.; Gotkin, P. J.; Kupfer, J. M.; Nafie, L. A. *J. Am. Chem. Soc.* **1978**, *100*, 5644. (b) Diem, M.; Photos, E.; Khouri, H.; Nafie, L. A. *J. Am. Chem. Soc.* **1979**, *101*, 6829. (c) Lal, B. B.; Diem, M.; Polavarapu, P. L.; Oboodi, M.; Freedman, T. B.; Nafie, L. A. *J. Am. Chem. Soc.* **1982**, *104*, 3336.
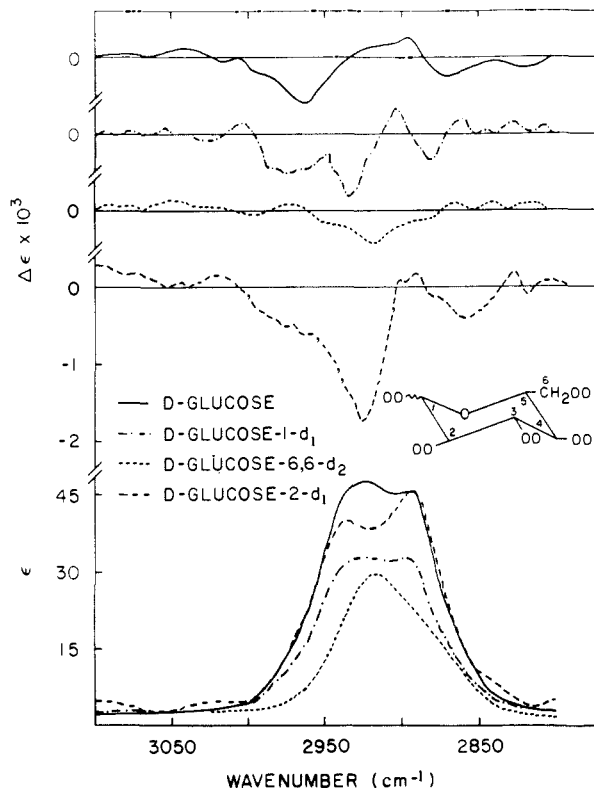

Figure 2. CH-stretching VCD and absorbance spectra of glucose isotopomers in D_2O. Concentration and path length conditions: D-glucose, 1.0 M, 0.11 mm; D-glucose-l-d_1, 0.5 M, 0.15 mm; D-glucose-6,6-d_2, 1.0 M, 0.11 mm; D-glucose-2-d_1, ~0.9 M, 0.05 mm.

Table I. Observed Frequencies and Intensities in the CH-Stretching Absorption and VCD Spectra of Selected Sugars

	IR		VCD	
sugar	frequency, cm^{-1}	ϵ_{max}, 10^3 cm^2 mol^{-1}	frequency, cm^{-1}	$10^3\Delta\epsilon_{max}$ 10^3 cm^2 mol^{-1}
D-glucose	2977 (sh)	12	2965	−0.6
	2930	46	2922	+0.2
	2895	45	2895	+0.3
			2975	−0.2
D-glucose-l-d_1	2977	9	2975	−0.5
	2930	31	2935	−0.8
			2904	+0.3
	2895	32		
			2885	−0.3
D-glucose-2-d_1	2975 (sh)	13	2975	
	2937	40		
			2925	−1.7
	2895	45		
			2860	−0.4
D-glucose-6,6-d_2	2918	29	2918	−0.4
	2886 (sh)	21		
D-mannose	2975 (sh)	17		
	2937	58		
			2925	−3.4
	2898	41		
D-gulose	2977 (sh)	10		
	2940	30		
	2918 (sh)	37		
	2905	40	2905	−1.5
D-xylose	2985	13	2985	−0.4
			2955	−0.9
	2935	32		
	2905	37	2900	−1.1
	2883 (sh)	29		
L-sorbose	2885	16	2885	−0.1
	2947	33	2952	+0.8
	2895	30	2900	+1.0

forms, in D_2O solution,[14-16] as shown in Table II. For the purpose of this analysis, the five-membered ring furanose and acylic forms

Vibrational Circular Dichroism of Sugars

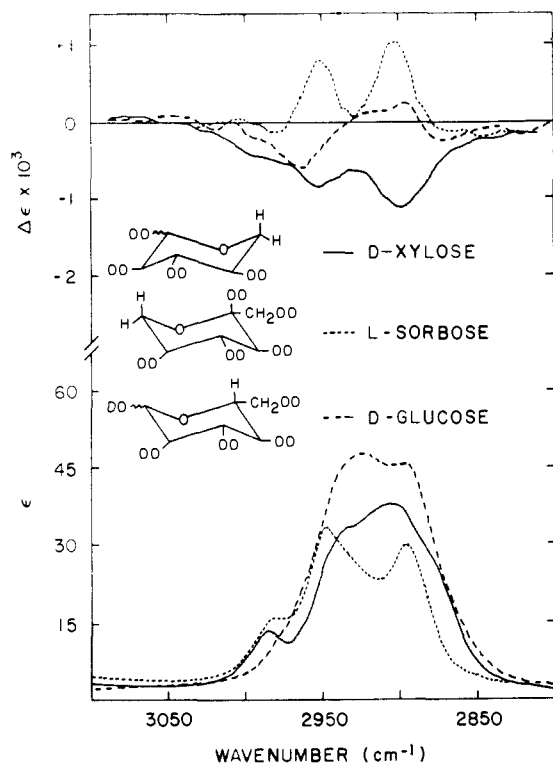*J. Am. Chem. Soc., Vol. 108, No. 7, 1986* 1391

Figure 3. CH-stretching VCD and absorbance spectra of D-xylose, L-sorbose, and D-glucose, in 1.0 M D_2O solution, 0.11-mm path length.

Table II. Equilibrium Percentages of Pyranose, Furanose, and Acyclic Forms of Several Sugars in D_2O Solution (24–44 °C)

	pyranose		furanose		
aldohexose	α	β	α	β	acyclic
D-glucose[a]	38	62	0	0	0.0002[b]
D-mannose[a]	65.5	34.5	0	0	0.005[b]
D-gulose[a]	16	78	6		0.02[c]
D-xylose[a]	39.5	63	<1		
L-sorbose[d]	92		2		

[a] Reference 14, from ^1H NMR. [b] Reference 15, from UVCD. [c] Estimated from UVCD spectra of D-glycero-D-guloheptose, ref 14. [d] Reference 16.

can be neglected. For the D-pyranose anomers investigated here, the C1 chair form is more stable, with the exception of α-D-gulopyranose, for which the C1 and 1C chair forms have similar energies.[17] Since only 16% of the gulose molecules is present as the α-anomer, our interpretation is based on the C1 forms for all the D enantiomers and the 1C form for L-sorbose.

Frequency Assignments. In order to interpret the CH-stretching VCD spectra in the sugars, an assignment of the absorption features is required, which can be deduced from a comparison of the spectra of various sugars and from the effects of specific deuteration. Since interactions among the local CH oscillators on individual carbon centers occur due to kinetic and potential energy coupling, the normal modes of the molecule are in fact combinations of various CH motions, and deuteration or inversion at a specific center can affect the frequencies, intensities, and internal coordinate contributions of the remaining normal modes. The assignments presented here serve primarily to locate the major contributions from local CH oscillators to the rather broad absorption features present in the solution spectra of sugars. Our analysis indicates that the dominant features can be ascribed to the motions of characteristic types of CH oscillators, the methylene group, or the methine in specific environments. The force constant, and thus the frequency, for a methine CH stretch depends on the

type and orientation of adjacent substituent groups with lone pairs or π electrons, such as hydroxyl, phenyl, or carboxylate. In solution, methine-stretching absorption features are often broadened due to a distribution in orientation of these substituents and fluctuations about the equilibrium conformations.[18]

The differences in the absorption spectra for the various sugars in Figure 1 are largely due to the different percentages of anomeric forms and to the different stretching frequencies for axial and equatorial methine bonds. The stretching frequencies for the anomeric α-CH (equatorial) and β-CH (axial) bonds in D-glucose have been assigned at 2948 cm⁻¹ (α) and 2884 cm⁻¹ (β) based on FTIR difference spectra for α- and β-D-glucose before and after equilibration in D_2O solution.[19] Since the anomeric concentration in mannose (65.5% α, 34.5% β) and glucose (38% α, 62% β) differ, the subtracted spectrum, D-mannose minus D-glucose, also provides an estimate of the C(1)H frequencies, a positive band at ~2944 cm⁻¹ in the difference spectrum corresponding to the excess of α-anomer in D-mannose, and a negative feature ~2880 cm⁻¹ corresponding to the excess of β-anomer in D-glucose.

The frequency of the axial C(2)H stretch obtained from the difference of the absorption spectra of D-glucose and D-glucose-2-d_1 (Figure 2) is 2923 cm⁻¹. Due to the similarity in their environments in solution, the stretching frequencies for axial C(2)H, C(3)H, and C(4)H are all expected to occur in the region near 2925 cm⁻¹. The equatorial methine CH stretch at carbons 2, 3, or 4 is assigned at 2905 cm⁻¹, based on the shift in the absorption maximum to 2905 cm⁻¹ for gulose, in which two methine bonds are equatorial, and on the gulose VCD feature at 2905 cm⁻¹, which can be attributed to an equatorial methine stretch (vide infra). A weak positive feature is also observed at 2905 cm⁻¹ in the D-mannose minus D-glucose subtraction, corresponding to the presence of the equatorial C(2)H bond in D-mannose but not in D-glucose.

A comparison of the absorption spectra for D-glucose and D-glucose-6,6-d_2 (Figure 2) reveals that the methylene C(6)H_2 modes contribute nearly half the total absorption intensity in the CH-stretching region. The difference of the absorption spectra for D-glucose and D-glucose-6,6-d_2 consist of two intense bands at 2937 and 2892 cm⁻¹ and a weaker shoulder at 2975 cm⁻¹. The high-frequency vibration clearly contributes negative VCD intensity at 2975 cm⁻¹ in the other glucose spectra, which is lost upon deuteration of the C(6) methylene hydrogens (Figure 2). This band is assigned to the antisymmetric methylene stretch. The bands at 2937 and 2892 cm⁻¹ are assigned to a Fermi resonance diad involving the symmetric CH_2 stretch and the overtone of the CH_2 scissors mode at 1458 cm⁻¹. The two components of the Fermi diad have nearly equal intensity, indicative of a strong resonance interaction.

The absorption corresponding to the C(5)H stretch is more difficult to locate, since a C(5)-d_1 isotope was not available for this study. Based on spectral simulations and analysis of the VCD spectra, to be discussed more fully below, the C(5)H frequency is assigned at ~2905 cm⁻¹. The frequency for the axial C(5)H, which lies adjacent to the ring oxygen, occurs at the mean of the frequencies for the axial β-C(1)H (2880 cm⁻¹), which is adjacent to both a ring C–O bond and a hydroxyl substituent C–O bond, and the frequency for axial C(2)H (2925 cm⁻¹), which is adjacent only to a hydroxyl substituent C–O bond.

D-Xylose and L-sorbose both have a methylene group within the pyranose ring. The antisymmetric ring CH_2 stretch occurs as a resolved band at 2985 cm⁻¹. The symmetric ring methylene stretch occurs as a Fermi resonance diad (with the CH_2 scissors overtone) at ~2950 and ~2900 cm⁻¹, as indicated by features in the absorption and VCD spectra (vide infra).

Spectral Simulations. The contributions from the individual modes to the total CH-stretching spectrum of D-glucose can be estimated by spectral simulation using a curve analysis program. Individual bands with 75% Lorentzian/25% Gaussian character

(14) Angyal, S. J.; Pickles, V. A. *Aust. J. Chem.* **1972**, *25*, 1695.
(15) Hayward, L. D.; Angyal, S. J. *Carbohydr. Res.* **1977**, *53*, 13.
(16) Angyal, S. J.; Bethell, G. S. *Aust. J. Chem.* **1976**, *29*, 1249.
(17) Angyal, S. J. *Angew. Chem., Int. Ed. Engl.* **1969**, *8*, 157.

(18) Cavagnat, D.; Lascombe, J. *J. Chem. Phys.* **1982**, *76*, 4336.
(19) Back, D. M.; Michalska, D. F.; Polavarapu, P. L. *Appl. Spectros.* **1984**, *38*, 173.

1392 *J. Am. Chem. Soc., Vol. 108, No. 7, 1986*

Paterlini et al.

Table III. Frequencies, Intensities, Half-Widths, and Assignments for the Component Bands in the Simulation of the D-Glucose CH-Stretching Absorbance Spectrum in Figure 4

band	frequency, cm^{-1}	half-width,[a] cm^{-1}	ϵ_{max}, 10^3 cm^2 mol^{-1}	dipole strength, 10^{-39} esu^2 cm^2	assignment
A	2975	26	1.6	0.4	$C(6)H_2^{asym}$
B	2949	24	13.3	2.8	α-C(1)H
C	2936	22.5	19.6	3.8	$C(6)H_2^{sym}(F.R)$[b]
D	2923	24	12.3	2.6	C(2)H, C(3)H, C(4)H
E	2909	24	6.0	1.3	C(5)H
F	2894	22.5	19.6	3.9	$C(6)H_2^{sym}(F.R.)$[b]
G	2888	24	11.7	2.5	β-C(1)H

[a] Half-width at $\epsilon_{max}/2$; bands are 25% Gaussian, 75% Lorentzian. [b] Fermi diad due to resonance between $C(6)H_2$ symmetric stretch and $C(6)H_2$ scissors overtone.
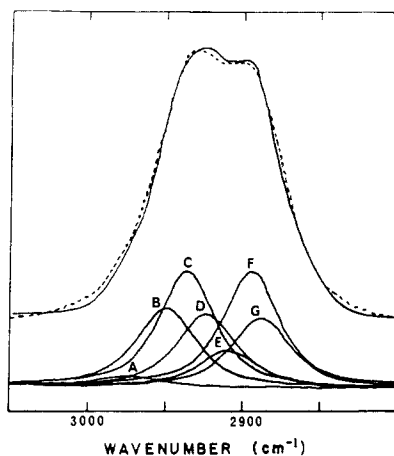
Figure 4. Comparison of the experimental absorbance spectrum (—) of D-glucose in D_2O with the spectral simulation (---) obtained by adding the individual component bands A–G. The frequencies, intensities, band widths, and assignments of components are listed in Table III.

were chosen, based on a fit to the lone C(2)H band obtained from the D-glucose minus D-glucose-2-d_1 subtraction. A methine band half-width of 25 cm^{-1} was also obtained from the C(2)H band simulation, and half-widths of 26 cm^{-1} for the antisymmetric $C(6)H_2$ mode and 22.5 cm^{-1} for the symmetric $C(6)H_2$ modes were obtained by fitting the D-glucose minus D-glucose-6,6-d_2 difference spectrum. The simulated spectrum in Figure 4 and Table III was obtained by locating bands with the above line shape and width at the frequencies assigned for individual modes and adjusting the intensities and making minor variations in frequencies until the closest fit to the observed spectrum was obtained. A single band for the C(2)H, C(3)H, and C(4)H modes was used, since the individual contributions from these modes cannot be accurately obtained from our data. A band at 2909 cm^{-1} for the C(5)H stretch was required for the best simulated fit. In agreement with the previously described comparisons among the spectra in Figures 1 and 2, the simulated glucose spectrum indicates that nearly half of the absorption intensity is due to the $C(6)H_2$ stretches and 30% is due to the anomeric C(1)H stretch, while only 15% of the total is due to methines C(2)H, C(3)H, and C(4)H. Based on the known anomeric composition in D-glucose solution ($\sim^2/_3\beta$, $\sim^1/_3\alpha$), ϵ_{max} values for the pure α- and β-anomers, 39.9 and 17.5 × 10^3 cm^2 mol^{-1}, respectively, are determined. The larger intensity and higher frequency for the α-C(1)H mode has been related to the orientation of the C(1)H bond relative to the lone pairs on the ring oxygen, since both of the lone pairs are gauche to the α-CH whereas one lone pair is trans and one gauche to the β-CH bond.[20-22]

VCD Assignments. The VCD maxima for the intense negative features in the VCD spectra of D-mannose, D-gulose, and D-glucose-2-d_1 (Figure 1) occur in the frequency region for the methine stretch at C(2), C(3), C(4), and C(5). More detailed

assignments for these features will be addressed in the Discussion section. In D-glucose (Figure 2), the intense negative feature is absent, and only weak VCD features of alternating sign remain. Since the $C(6)H_2$ symmetric stretching Fermi diad and the α-C(1)H and β-C(1)H absorption bands occur near the same frequencies, assignments of VCD due to $C(6)H_2$ are best obtained from the D-glucose-1-d_1 spectrum. Negative features at 2975, 2935, and 2885 cm^{-1} are observed, corresponding to the antisymmetric and symmetric stretching frequencies for the $C(6)H_2$ group. We assign a positive feature at 2905 cm^{-1} to the C(5)H stretch. All four of these features are absent in the D-glucose-6,6-d_2 VCD spectrum. Comparison of the D-glucose and D-glucose-1-d_1 spectra indicates that the α-C(1)H stretch contributes positive VCD at $\sim$2945 cm^{-1} which nearly cancels the negative VCD due to the $C(6)H_2$ mode at $\sim$2935 cm^{-1}. The contribution from the β-C(1)H stretch at $\sim$2885 cm^{-1} appears to be negligible. The VCD of D-glucose-6,6-d_2, the sum of the five methine contributions, consists of broad weak negative VCD centered at 2920 cm^{-1}.

IV. Discussion

Ring Current Mechanism. Vibrational circular dichroism intensity is proportional to the rotational strength $R_{10} = Im(\mu_{01} \cdot m_{10})$ where μ_{01} is the electric dipole transition moment and m_{10}, the magnetic dipole transition moment for a fundamental 0 → 1 transition. To generate VCD, a normal mode of vibration, Q_a, with conjugate momentum, P_a, must simultaneously produce a linear oscillation of charge, $(\partial\mu/\partial Q_a)_0$, and an angular or circular oscillation of charge, $(\partial m/\partial P_a)_0$.[2-4,9] The magnetic dipole contribution has been proposed to arise from two effects: (1) the chiral orientation of two or more local oscillating electric moments on different centers as described by the coupled oscillator[23] and fixed partial charge (FPC)[24] models, where the electronic motion perfectly follows the nuclear motion, and (2) oscillating electronic charge flow along groups of bonds or around a ring which is generated by the nuclear motion but is distinct from it. The latter effects are described by the charge flow model[25,26] for charge flow along bonds leading to a redistribution of electron density, and additional contributions due to the ring current mechanism,[9] wherein the nuclear momenta generate electron flow around a closed ring at constant electron density. In the CH-stretching region, where the normal modes do not contain significant contributions from lower frequency motions, the coupled oscillator mechanism leads to VCD with no net bias (integrated intensity over the CH-stretching region), whereas bond charge flow and ring current can lead to biased VCD.

The specific mechanism proposed for the ring current enhancement of methine-stretching modes is due to an oscillator external to a ring (rule 1),[4-7,9] described as follows: contraction of the CH oscillator injects electrons into the hydrogen-bonded ring preferentially toward the bond with less tightly held electron density, which for the cases considered here is the bond to the heteroatom, C^*-X. Due to the closed ring pathway, positive current flow around the ring is generated which gives rise to a

(20) McKean, D. C. *Chem. Soc. Rev.* **1978**, *1*, 399.
(21) Krueger, P. J.; Jan, J.; Wieser, H. *J. Mol. Struct.* **1970**, *5*, 375.
(22) Caillod, J.; Saur, O.; Lavelley, J.-C. *Spectrochim. Acta, Part A* **1980**, *36A*, 185.

(23) Holzwarth, G.; Chabay, E. *J. Chem. Phys.* **1972**, *57*, 1632.
(24) Schellman, J. A. *J. Chem. Phys.* **1973**, *58*, 2882; **1974**, *60*, 343.
(25) Moskovits, M.; Gohin, A. *J. Phys. Chem.* **1982**, *86*, 3947.
(26) Abbate, S.; Laux, L.; Overend, J.; Moscowitz, A. *J. Chem. Phys.* **1981**, *75*, 3161.

Vibrational Circular Dichroism of Sugars

J. Am. Chem. Soc., Vol. 108, No. 7, 1986 1393

magnetic dipole moment **m**. CH contraction results in an electric dipole moment μ directed C $\rightarrow$ H. CH elongation reverses the sense of both moments, since electrons are now preferentially withdrawn from the C–X bond. The scalar product of these oscillating electric and magnetic dipole moments due to the methine vibration produces VCD intensity, which is positive for the configuration **1**, shown for CH contraction.

1
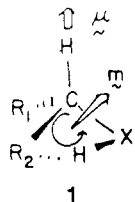
In the sugars, numerous intramolecularly hydrogen-bonded rings are possible, joining either two hydroxyl substituents or a hydroxyl group and the ring oxygen. Current around the pyranose ring itself is also possible. In D_2O solution, the sugar conformations are present as an equilibrium among various bonded and free forms.

Our analysis of the large VCD bias observed for some of the sugars is based on intrinsic contributions from the individual methine-stretching modes due to ring current in adjacent rings. The methine motions occur in a fairly restricted frequency range, and the actual normal modes no doubt contain contributions from several CH oscillators. When adjacent CH bonds are chirally oriented, contributions to the VCD from coupled CH motions are also possible, but since the various methine modes are not resolved in solution, these coupling contributions will largely cancel, and therefore knowledge of the precise descriptions of the normal modes is not necessary. In analyzing the CH-stretching VCD as a sum of individual intrinsic methine contributions, we assume that all possible intramolecularly hydrogen bonded rings are equally probable, and that intrinsic methine VCD is negligible when an adjacent ring is absent, as observed for α-phenylethane derivatives.[7] Since reduction in the concentration does not affect the anisotropy ratio for the 2925-cm^{-1} band in D-mannose, any intermolecular associations among sugar molecules appear not to be contributing to the VCD.

CH Stretching at Carbon 2, 3, and 4. The glucose, glucose-*1-d₁*, and glucose-*6,6-d₂* VCD spectra (Figure 2) demonstrate that the VCD contributions due to C(1)H, C(6)H₂, and most likely C(5)H are relatively small and therefore our interpretation will initially focus on the remaining three methine modes and the hydrogen-bonded rings joining carbons 2, 3, and 4. For D-mannose, D-glucose, D-glucose-*2-d₁*, and D-gulose, the contributions to the VCD from C(2)H, C(3)H, and C(4)H contractions are illustrated in Figure 5. In D-mannose, the C(2)H bond is equatorial and is adjacent to a hydrogen-bonded ring joining the hydroxyl groups at carbons 2 and 3. (Although the ring is drawn with the deuterium donor from the C(3)OD, the VCD contribution is equivalent for a ring originating from C(2)OD⋯OC(3) interaction.) Contraction of C(2)H gives rise to the electric moment μ_2 and generates positive current around the ring in the direction O $\rightarrow$ C(2) and the magnetic moment **m₂** in the illustration. Since the methine C(2)H bond is approximately orthogonal to the plane of the ring, μ_2 and **m₂** are nearly antiparallel, giving rise to strong negative VCD with a magnitude denoted as $R_2 = -\Delta$. The axial methine C(3)H bond is adjacent to two rings $\overline{C(3)OD\cdots OC(2)}$ and $\overline{C(3)O\cdots DOC(4)}$. (Again the source of the deuterium in the bond is irrelevant.) C(3)H contraction gives rise to the electric moment μ_3 and ring currents in both rings, leading to magnetic moments **m₃** and **m₃'**. The C(3)H bond lies approximately in the plane of the ring joining carbons 2 and 3, resulting in nearly orthogonal μ_3 and **m₃'**, and $\mu_3 \cdot$**m₃'** ≈ 0. Since the C(3)H bond is orthogonal to the plane of the ring joining carbons 3 and 4, positive ring current in this ring leads to antiparallel μ_3 and **m₃** and intrinsic contribution $R_3 \approx -\Delta$. The axial C(4)H bond is also orthogonal to the plane of the ring joining carbons 3 and 4, and positive ring current in the direction O $\rightarrow$ C(4) again leads to a

contribution $R_4 = -\Delta$. The total predicted rotational strength in D-mannose due to vibrationally generated ring currents in the rings joining carbons 2, 3, and 4 is therefore $R_T = -3\Delta$. We note that when the individual methine motions are phased to form the normal modes, the currents in the two rings can either be reinforced due to additive contributions or diminished due to opposing current contributions. As a result, the intrinsic VCD contributions will be distributed among the normal modes. Since C(2)H is chirally oriented relative to C(3)H and C(4)H, VCD due to coupled methine motions also occurs in mannose but would be observed as unbiased oppositely signed contributions from variously phased motions. The observed D-mannose CH-stretching VCD is totally negatively biased, in agreement with the prediction of the ring current mechanism and indicating that any coupled oscillator contributions are not significant.

In D-glucose, C(2)H, C(3)H, and C(4)H are all axial, and each bond is orthogonal to the adjacent intramolecularly hydrogen-bonded ring (or rings) joining these carbon centers. All the moments are therefore parallel or antiparallel. As diagrammed in Figure 5, the intrinsic rotational strength contributions arising from vibrationally generated ring current are $R_2 = +\Delta$, $R_3 = 0$, and $R_4 = -\Delta$, since contractions of C(2)H and C(4)H leads to magnetic moments in the opposite direction, whereas for C(3)H contraction opposing magnetic moments due to currents generated in the two adjacent rings lead to no net rotational strength. The total predicted rotational strength for glucose due to the ring currents in the rings joining carbons 2, 3, and 4 is zero. The observed CH-stretching VCD spectrum of D-glucose (Figure 2) is considerably smaller than that of D-mannose, and the VCD features which are present can be attributed to other CH-stretching modes or other rings, as discussed below.

In D-glucose-*2-d₁*, the contribution from the methine C(2)D stretch, R_2, is shifted to $\sim$2200 cm^{-1}. In the CH-stretching region, a net rotational strength $R_T = -\Delta$ is therefore predicted due to R_4. The major VCD feature of D-glucose-*2-d₁* is a negative band centered at 2925 cm^{-1}. The integrated intensities for the large negative features in D-mannose and D-glucose-*2-d₁* lead to observed rotational strengths (Table IV) in a ratio approximately 3:1, as predicted by the ring current mechanism.

In D-gulose, C(2)H is axial and C(3)H and C(4)H are equatorial. Due to the trans arrangement of the OD groups at C(3) and C(4), no intramolecularly hydrogen-bonded ring joining these two carbons is possible. The C(2)H bond lies approximately in the plane of the ring joining carbons 2 and 3, whereas the C(3)H bond is orthogonal to this plane. As a result, $R_2 = 0$ due to orthogonal μ_2 and **m₂**, $R_3 = -\Delta$ due to antiparallel μ_3 and **m₃**, and $R_4 = 0$ since no adjacent ring is present (**m₄** = 0). A net rotational strength due to ring currents $R_T = -\Delta$ is predicted for D-gulose. The observed CH-stretching VCD (Figure 1) consists of a single negative feature centered at 2905 cm^{-1}. The observed rotational strength of this band (Table IV) is approximately 1/3 that of D-mannose, again in agreement with the prediction of the ring current mechanism.

The difference in the position of the VCD features in Figure 1 is also explained by this analysis. In D-glucose-*2-d₁*, the VCD arises from the intrinsic contribution from an axial CH stretch, assigned at 2925 cm^{-1}; in D-gulose, the VCD arises from a single equatorial CH stretch at 2905 cm^{-1}, and in D-mannose, the VCD arises from equivalent contributions from two axial CH stretches and one equatorial CH stretch and occurs as a broad band encompassing both regions, but centered at 2925 cm^{-1}. The value of Δ determined from these spectra is 5.8 × 10^{-44} esu^2 cm^2. Assuming equal contributions from C(2)H, C(3)H, and C(4)H

CH STRETCHING VCD DUE TO RING CURRENT
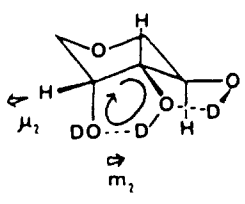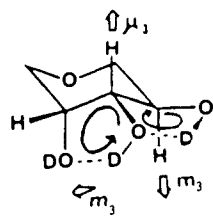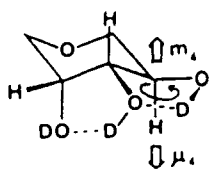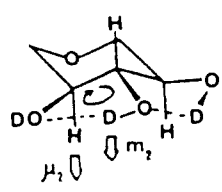## IN HYDROGEN - BONDED RINGS JOINING CARBONS 2, 3 AND 4
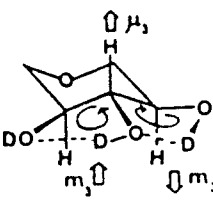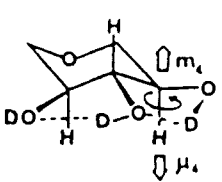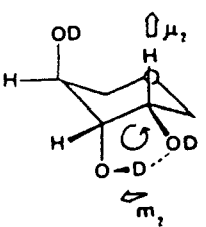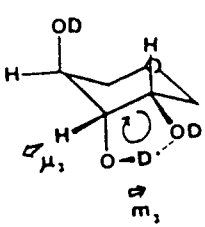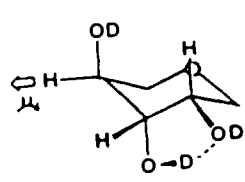

BOND CONTRACTION

| C (2) H | C (3) H | C (4) H |

$R_2 = -\Delta$

$\nu = 2905$ cm^{-1}

$R_3 = -\Delta$

$\nu = 2925$ cm^{-1}

$R_4 = -\Delta$

$\nu = 2925$ cm^{-1}

D-MANNOSE   Predicted Rotational Strength = - 3Δ

$R_2 = +\Delta$

$\nu = 2925$ cm^{-1}

$R_3 = +\Delta - \Delta = 0$

$\nu = 2925$ cm^{-1}

$R_4 = -\Delta$

$\nu = 2925$ cm^{-1}

D-GLUCOSE   Predicted Rotational Strength = 0

D-GLUCOSE-2-d$_1$ = -Δ

$R_2 = 0$

$R_3 = -\Delta$

$R_4 = 0$

$\nu = 2905$ cm^{-1}

D-GULOSE   Predicted Rotational Strength = - Δ

Figure 5. Intrinsic VCD contributions from C(2)H, C(3)H, and C(4)H methine stretch in D-mannose, D-glucose, D-glucose-2-d$_1$, and D-gulose due to vibrationally generated currents in the hydrogen-bonded rings joining carbons 2, 3, and 4.

stretches to the absorption band at 2923 cm^{-1} obtained from the spectral simulation of the D-glucose absorbance spectrum (Figure 4), the magnitude of the anisotropy ratio $g = 4R/D$ for ring current enhanced methine VCD in the sugars is $\sim$2.7 × 10^{-4}, similar to that observed for the enhanced methine stretch in amino acids and α-hydroxy acids and esters.[5-7]

The magnetic dipole transition moment due to ring current is proportional to[9]

$$\left(\frac{\partial m^{ring}}{\partial P_a}\right)_{0,0} = \frac{1}{c}\left(\frac{\partial \Gamma^{ring}}{\partial P_a}\right)_{0,0^{n-12}}\sum_{}^{ring}\frac{1}{2}R_{n,0} \times R_{l,0} \qquad (1)$$

where $(\partial \Gamma^{ring}/\partial P_a)_{0,0}$ is the vibrationally generated current about the ring and the summation is taken around the ring in the di-

rection of positive current for all pairs of atoms n and l at equilibrium positions $R_{n,0}$ and $R_{l,0}$. For D-glucose-2-d$_1$, assuming μ_4 to lie along C(4)H, the angle between μ_4 and m$_4$ is $\sim$160°, and the current $(\partial \Gamma^{ring}/\partial P_a)_0$ is 0.004 electrons per vibrational half cycle, comparable to that found for current generated by the methine stretch in amino acids and α-hydroxy acids but smaller than that observed for currents generated by NH stretching.[8]

Methylene Stretch at Carbon 5. The strongly biased CH-stretching VCD in D-xylose and L-sorbose (Figure 3) can also be interpreted in terms of the ring current mechanism. In both molecules, C(2)H, C(3)H, and C(4)H are all axial, and in analogy to the interpretation for D-glucose, no ring current VCD due to the stretching motions of the methines and the hydrogen-bonded rings joining carbons 2, 3, and 4 is predicted. Compared to glucose,
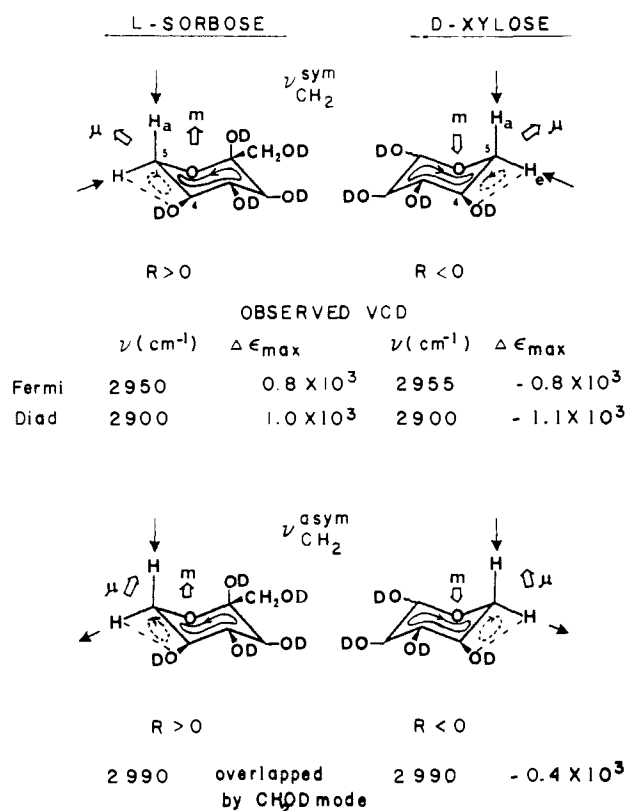
Vibrational Circular Dichroism of Sugars

J. Am. Chem. Soc., Vol. 108, No. 7, 1986 1395

RING CURRENT MECHANISM FOR
C(5) METHYLENE STRETCHING MODES

OBSERVED VCD

	ν (cm^{-1})	$\Delta \epsilon_{max}$	ν (cm^{-1})	$\Delta \epsilon_{max}$
Fermi	2950	0.8 X 10^3	2955	- 0.8 X 10^3
Diad	2900	1.0 X 10^3	2900	- 1.1 X 10^3

| 2990 | overlapped by CH$_2$OD mode | 2990 | - 0.4 X 10^3 |

Figure 6. Intrinsic VCD contributions for the C(5)H$_2$ methylene symmetric and antisymmetric stretching modes in L-sorbose and D-xylose due to vibrationally generated ring currents.

in both xylose and sorbose, the CH$_2$OD substituent at C(5) is replaced by a hydrogen. In sorbose, a CH$_2$OD group replaces the anomeric hydrogen at C(1) in glucose.

The VCD maxima in L-sorbose and D-xylose at ~2950 and 2900 cm^{-1} correspond to the frequencies expected for the Fermi diad involving the symmetric stretch of the ring methylene group and the overtone of the methylene scissors mode. As illustrated in Figure 6, the most favorable pyranose conformations of L-sorbose (1C) and D-xylose (C1) are mirror images, with the exception of the C(1) substituents. The symmetric methylene C(5)H$_2$ contraction in both molecules results in an electric dipole moment μ having an upward component in the diagram. Since the methylene lies adjacent to the ring oxygen, the contraction of each methylene C(5)H bond injects electrons preferentially toward the ring oxygen, relative to the C(5)–C(4) bond, leading to positive current around the pyranose ring, producing a magnetic dipole moment directed upward for L-sorbose and downward for D-xylose. The predicted mirror image negative VCD for D-xylose and positive VCD for L-sorbose is observed as features of the predicted sign at ~2950 and 2900 cm^{-1}, with nearly equal and opposite $\Delta\epsilon_{max}$ for the two sugars.

The negative VCD observed at 2990 cm^{-1} in D-xylose corresponds to the antisymmetric methylene stretch. From the ring current mechanism, negative VCD in the antisymmetric methylene stretch requires that the magnetic moments due to currents resulting from axial methylene C(5)H contraction and the equatorial C(5)H elongation do not cancel and that the magnetic moment due to the *axial* C(5)H dominates. This could occur if the axial C(5)H bond has the higher force constant and therefore the larger contribution to the higher frequency antisymmetric methylene stretch. In L-sorbose, a similar positive VCD predicted for the antisymmetric methylene stretch is apparently canceled by a negative contribution from the CH$_2$OD antisymmetric stretching mode, as observed at 2975 cm^{-1} for D-glucose.

This explanation for the antisymmetric methylene-stretching VCD is not entirely satisfactory, since the α-C(1)H (equatorial) stretching frequency is higher than that of the β-C(1)H (axial) stretch. Alternatively, the magnetic contribution from the motion of the equatorial CH bond of the methylene may be diminished due to the second rule for ring current generation due to an oscillator within a ring,[4,7,8] which has been deduced from the enhancement of methyl-,[7] amino-,[8] and hydroxyl-stretching[7] modes when a CH, NH, or OH bond is near a π orbital or lone pair. In sorbose and xylose, the equatorial, but not the axial, methylene C(5)H bond can interact with a lone pair on the C(4)OD oxygen to produce an opposing magnetic contribution. The equatorial C(5)H interaction is indicated by the dashed line in Figure 6. Elongation of the equatorial C(5)H bond strengthens the hydrogen bond, drawing electrons from the oxygen, while equatorial C(5)H contraction weakens the interaction, causing electrons to flow back to the oxygen. The positive ring currents initiated due to the C(5)H···O interaction, indicated by dotted circles in Figure 6, produce oscillating magnetic dipole moments which oppose the magnetic moments due to current around the pyranose ring also generated by the equatorial C(5)H bond. As a result, the contribution from the axial C(5)H stretch dominates in both the symmetric and antisymmetric stretching regions, giving rise to negative VCD for D-xylose and positive VCD for L-sorbose in both regions. The ring current contribution from the axial CH motion may also be larger due to the interaction between the axial CH and the trans lone pair on the ring oxygen.[20-22]

CH Stretching at Carbons 1, 5, and 6. The weaker VCD signals observed for glucose and the deuterated isotopomers in Figure 2 can also be largely attributed to vibrational ring current contributions. As noted in the Results section, a comparison of the VCD for D-glucose and D-glucose-*1-d$_1$* indicates that the anomeric α-C(1)H stretch exhibits positive VCD at ~2940, but any contribution from the β-C(1)H stretch, ~2885 cm^{-1}, is within the noise level of the experiment. The α-C(1)H contraction can generate current in the ring C(2)OD···OC(1) which gives rise to positive VCD as shown in **2a**. Since the α-C(1)H bond is

R > 0   R ~ 0

2a   **2b**
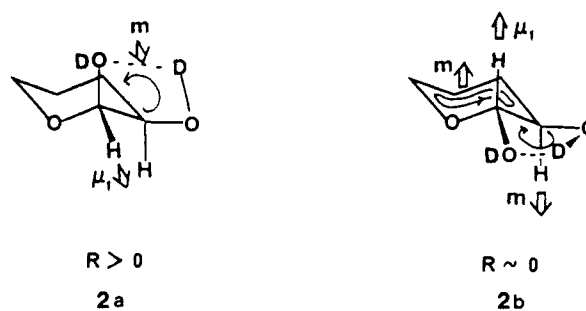
equatorial, the magnetic moment due to current generated around the adjacent pyranose ring is nearly orthogonal to μ for the α-C(1)H stretch and does not contribute to the VCD. The α-C(1)H-stretching VCD is weaker than that observed for the C(4)H stretch in D-glucose-*2-d$_1$* since the α-anomeric percentage is only 38%. The axial β-C(1)H contraction can generate current in both the pyranose ring and the C(2)OD···OC(1) ring, as shown in **2b**, giving rise to magnetic moments in opposite directions and little if any VCD, as observed.

The net negative VCD observed at ~2920 cm^{-1} in D-glucose-*6,6-d$_2$* can be attributed to methine C(2)-H-stretching enhancement due to current generated in the adjacent C(2)O-D···OC(1) ring for the β anomer **3a** but not in the α-anomer **3b** in which μ_2 and m$_2$ are orthogonal.

Both the symmetric and antisymmetric C(6)H$_2$ methylene modes exhibit negative VCD, whereas the positive VCD attributed to the C(5)H mode observed at ~2905 in D-glucose, D-glucose-*1-d$_1$*, and D-glucose-*2-d$_1$* is absent in D-glucose-*6,6-d$_2$*. The C(6)H$_2$ group can assume three rotameric conformations about the C-(6)–C(5) bond, **4a–c**, shown as Newman projections for the symmetric methylene contraction. H$_a$ and H$_e$ denote the CH

R < 0   R ~ 0

3a   3b

R > 0   R < 0   R < 0

4a   4b   4c
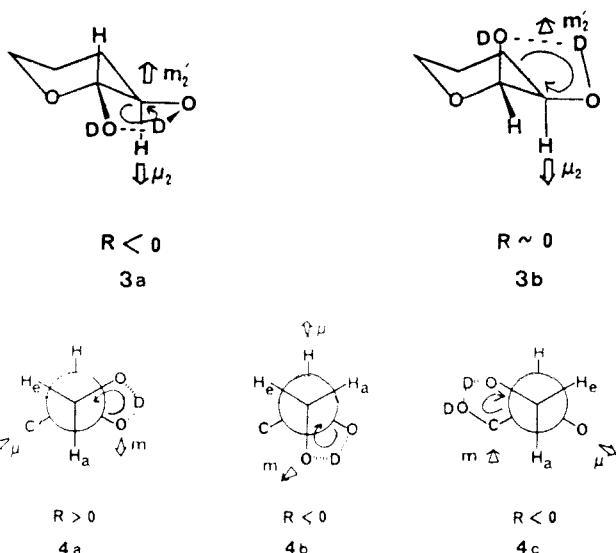
bond axial or equatorial relative to the adjacent hydrogen-bonded ring. In **4a** and **4b**, a hydrogen bond to the ring oxygen forms a five-membered ring, whereas in **4c** a hydrogen bond to the –OD group at C(4) forms a six-membered ring. Assuming approximately equal populations of the five-membered ring forms **4a** and **4b**, which therefore cancel, a net negative VCD for the symmetric $C(6)H_2$-stretching mode due to **4c** is predicted, as observed. The negative VCD for the antisymmetric $C(6)H_2$ mode again requires a larger ring current contribution from the axial C(6)H bond, implying a larger force constant compared to the equatorial C(6)H. This latter effect is consistent with the difference in the methine force constant observed for axial vs. equatorial CH at carbons 2, 3, and 4. Alternatively, the interaction between the equatorial C(6)H bond and the pyranose ring oxygen in **4c** can reduce the magnetic dipole contribution from the equatorial C(6)H motion, in a manner analogous to the interpretation above for sorbose and xylose.

The C(5)H contraction produces current around the pyranose ring which is predicted to give rise to a negative VCD contribution. This effect may be partially cancelled by a positive ring current VCD due to the adjacent ring to C(6)H for the conformer in **4a**. An additional source of VCD intensity is required to explain the positive C(5)H-stretching VCD when $C(6)H_2$ is present. In conformers **4a** and **4c**, the C(5)H and $C(6)H_2$ groups are chirally oriented, and coupling among the vibrations of the two groups can generate VCD. The unperturbed symmetric CH_2 stretch, predicted to occur near 2920 cm^{-1}, can mix with the methine C(5)H mode, located near 2909 cm^{-1} in the simulated absorption spectrum. Model normal coordinate calculations predict that the coupled modes **5a** and **5b** occur for the conformer in **4c**, with positive VCD for the mode with the larger methine contribution **5b**. Since the mirror image CH_2CH orientations in **4a** and **4c**

higher frequency   lower frequency
negative VCD   positive VCD

5a   5b
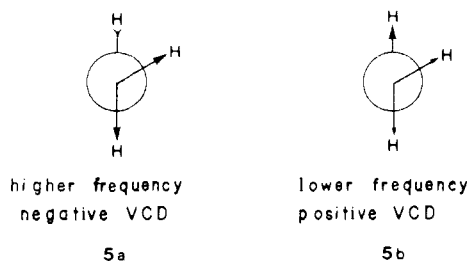
generate oppositely signed coupled oscillator VCD, this analysis indicates a larger percentage of conformer **4c**, possibly resulting from a stronger hydrogen bond to a hydroxyl oxygen compared to an ether oxygen. This source of positive VCD for the C(5)H stretch is removed upon deuteration at C(6), consistent with the observed VCD results. This coupled oscillator mechanism generates additional negative VCD for the symmetric methylene-stretching mode but cannot be the sole source of the VCD for the

$C(6)H_2$ group, since the antisymmetric $C(6)H_2$ mode is too high in frequency to couple with the C(5)H stretch, and the D-glucose-1-d_2 VCD is quite negatively biased.

VCD in Other Sugars. Both the sign and relative magnitudes of the VCD for the additional pyranose sugars surveyed by Havel[11] can be consistently interpreted in terms of the ring current mechanism. For sugars with a symmetric arrangement of substituents at C(2) and C(4) relative to a plane bisecting the ring through the ring oxygen and C(3), the ring current contributions due to rings joining carbons 2, 3, and 4 cancel, analogous to the interpretation above for D-glucose. Sugars in this class include the aldohexoses D-glucose, D-allose, D-talose, and D-idose for which only very weak VCD was observed. Sugars which lack this symmetry at C(2) and C(4), but which have gauche OD bonds at carbons 2, 3, and 4, have adjacent hydrogen-bonded rings for which the ring current contributions do not cancel, analogous to the interpretation above for D-mannose. Sugars in this class include D-mannose, D-galactose, 6-deoxy-L-mannose, 6-deoxy-D-galactose, D-arabinose, D-lyxose, D-fructose, and D-tagatose for which large monosignate VCD was reported. In solutions of D-gulose and D-altrose, most of the molecules assume a C1 chair form for which two adjacent OD bonds at C(2), C(3), and C(4) are trans, eliminating one of the two rings joining these three carbons. As described above for D-gulose, the VCD in both these sugars is about $^1/_3$ the magnitude of the VCD measured for D-mannose. Additional VCD contributions which can be attributed to a ring methylene group are also observed for the aldopentoses and 2-ketohexoses surveyed.

As a final example of ring current enhanced VCD, we return to the first reported VCD in sugars, α-methyl D-glucoside and β-methyl D-glucoside, which exhibit approximately mirror image VCD spectra ascribed to the OCH_3 group. In particular, bands at ~2905 and ~2850 cm^{-1} (positive for the α-anomer) were observed, which can be assigned to the Fermi diad involving the symmetric methyl stretch and the antisymmetric methyl deformation overtone.

In both anomers, a closed ring adjacent to the methoxy group is formed by interaction between the OD group at C(2) and the methoxy oxygen at C(1). This ring and the adjacent methyl group have a mirror image relationship in the α- and β-methyl D-glucosides, as illustrated in **6a** and **6b**. The symmetric methyl

R > 0   R < 0

6a   6b
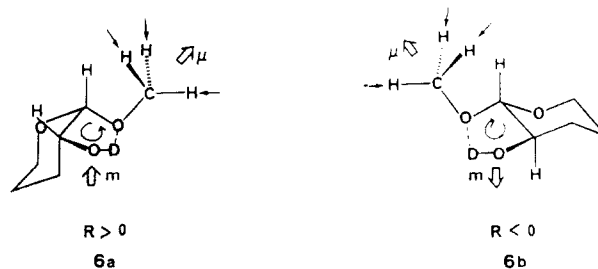
contraction injects electrons into the ring via the methoxy oxygen. According to the rule for preferred electron flow to the bond with less tightly held electron density, positive ring current is initiated in the direction C(2)OD → OC(1) which gives rise to positive ring current VCD for the α-anomer and negative ring current VCD for the β-anomer, as observed.

V. Conclusions

We have demonstrated that both the sign and relative magnitude of the CH-stretching VCD in a wide variety of pyranose sugars can be understood almost exclusively in terms of vibrationally generated ring currents. Any VCD arising from coupling among methine motions apparently cancels in D_2O solution due to only small frequency separations among the modes. In D-glucose, only the effects of methine–methylene coupling are observed, since Fermi resonance causes perturbation of the symmetric $C(6)H_2$-stretching mode and a significant shift in its frequency from the C(5)H stretch. The ring current model permits a complete interpretation of the CH-stretching VCD without a detailed knowledge of the precise nuclear contributions to each

normal mode, since the VCD intensities can be attributed to intrinsic contributions due to local oscillators. In applying the model, it is important to consider all possible rings including covalent, hydrogen-bonding, and alkyl/π or alkyl/lone pair interactions.

It is probable that the ring current mechanism is also important in generating the negative bias observed in the CH-stretching VCD of the aldohexose peracetates[11] and in the strong mid-infrared VCD band identified at $\sim$1150 cm^{-1} in Me$_2$SO-d_6 solutions of sugars.[12] Application of the model to the mid-infrared region requires a more accurate knowledge of the normal coordinates, since CC and CO stretches and CH deformation all contribute significantly.

The results of this study are significant from several points of view. First, a uniform explanation is provided for a broad class of VCD spectra. In addition, further evidence is established for the importance of the vibrational ring current intensity mechanism. Finally, this work forms a basis for a variety of stereochemical studies of sugars and related molecules in aqueous solution.

Theoretical Study of Carbanions and Lithium Salts Derived from Dimethyl Sulfone

Daniel A. Bors and Andrew Streitwieser, Jr.*

Contribution from the Department of Chemistry, University of California, Berkeley, California 94704. Received September 9, 1985

Abstract: Theoretical ab initio studies of the anion of dimethyl sulfone using a modified 3-21G(*) basis set with subsequent electron density analysis reveal that d-p π conjugation is not an important factor in stabilizing the anion. Instead, simple coulombic interactions play a dominant role with significant charge polarization. Optimization of the related lithium salt gives two minima on the potential surface with the lithium cation location determined by electrostatic effects. Optimization of the dilithium salts of dimethyl sulfone shows that the α,α-dianion is 9.30 kcal mol^{-1} less stable than the α,α'-dianion.

Any thorough analysis of the factors influencing the stability of carbanions adjacent to sulfur groups must invariably address the continuing controversy over the role of sulfur d-orbitals. Early theorists suggested that overlap of the lone pair orbital on the anionic carbon with the empty d-orbitals on sulfur provides stabilization of the anion through charge transfer.[1,2] Others, however, objecting to the idea of substantial d-p π-bonding, argued that the empty sulfur 3d-orbitals are too high in energy and too diffuse to interact with the carbon p-orbitals.[3] Recent studies by Wolfe suggest that sulfur d-orbitals are important in lowering the energy by n–σ* interaction.[4] Finally, charge polarization involving sulfur d-orbitals cannot be ruled out.[5d] While the subject is still debated, a consensus is forming among both theorists and experimentalists that sulfur d-orbitals have no substantial bonding interaction with α-carbanions for cases involving sulfides.[5]

For α-sulfinyl and α-sulfonyl compounds, on the other hand, the role of sulfur d-orbitals in the stabilization of carbanions is more controversial.[2,4,6] This is partly caused by the lack of

Table I. Optimized Geometries of Dimethyl Sulfone[a]

	3-21G	3-21G(*)	exptl
energy, au	−623.03238	−623.30361	
Bond Lengths, Å			
S–O	1.592	1.438	1.431
S–C	1.831	1.756	1.777
C–H$_t$	1.079	1.083	
C–H	1.078	1.080	
Angles, deg			
O–S–O	119.1	119.5	121.0
C–S–C	102.7	102.8	103.3
H–C–H	112.2	110.4	
H$_t$–C–S	106.8	107.6	
S–(HCH)[b]	124.4	127.9	

[a] Data taken from ref 13. C_{2V} symmetry assumed in all cases. Subscript t refers to the hydrogen that lies in the plane of symmetry. [b] Nomenclature signifies the angle between the first atom and the plane formed by the atoms in parenthesis.

sophisticated theoretical studies of these large molecular systems. Consequently, to provide more insight into this specific area, theoretical studies were performed on the anion of dimethyl sulfone. Analysis of the role of d-orbitals on the sulfur atom in

(1) (a) Mitchell, K. A. R. *Chem. Rev.* **1974,** *69,* 157. (b) Sidgwick, N. V. "The Electronic Theory of Valency"; Clarendon Press: Oxford, 1977.

(2) (a) Craig, D. P. *J. Chem. Soc.* **1956,** 4895. (b) Doering, W. E.; Levy, L. K. *J. Am. Chem. Soc.* **1955,** *77,* 509. (c) Zimmerman, H. E.; Thyagarajan, B. S. *J. Am. Chem. Soc.* **1960,** *82,* 2505.

(3) (a) Cilento, G. *Chem. Rev.* **1960,** *60,* 147. (b) Coulson, C. A. *Nature (London)* **1969,** *221,* 1106.

(4) Wolfe, S.; Stolow, A.; LaJohn, L. A. *Tetrahedron Lett.* **1983,** *24,* 4071.

(5) (a) Borden, W. T.; Davidson, E. R.; Andersen, N. H.; Denniston, A. D.; Epiotis, N. D. *J. Am. Chem. Soc.* **1978,** *100,* 1604. (b) Epiotis, N. D.; Yates, R. L.; Bernardi, F.; Wolfe, S. *J. Am. Chem. Soc.* **1976,** *98,* 5435. (c) Lehn, J. M.; Wipff, G. *J. Am. Chem. Soc.* **1976,** *98,* 7498. (d) Streitwieser, A., Jr.; Williams, J. E., Jr. *J. Am. Chem. Soc.* **1975,** *97,* 191. (e) Bernardi, F.; Csizmadia, I. G.; Mangini, A.; Schlegel, H. B.; Whangbo, M. H.; Wolfe, S. *J. Am. Chem. Soc.* **1975,** *97,* 2209. (f) Lehn, J. M.; Wipff, G.; Demuynck, J., *Helv. Chim. Acta.* **1977,** *60,* 1239. (g) Wolfe, S.; LaJohn, L. A.; Bernardi, F.; Mangini, A.; Tonachini, G. *Tetrahedron Lett.* **1983,** *24,* 3789.

(6) (a) Corey, E. J.; Konig, H.; Lowry, T. H. *Tetrahedron Lett.* **1962,** 515. (b) Corey, E. J.; Lowry, T. H. *Tetrahedron Lett.* **1975,** 793. (c) Corey, E. J.; Lowry, T. H. *Tetrahedron Lett.* **1965,** 803. (d) Roitman, J. N.; Cram, D. J. *J. Am. Chem. Soc.* **1971,** *93,* 2225. (e) Bordwell, F. G.; Branca, J. C.; Johnson, C. R.; Vanier, N. R. *J. Org. Chem.* **1980,** *45,* 3884. (f) Lett, R.; Chassaing, G. *Tetrahedron* **1978,** *34,* 2505. (g) Chassaing, G.; Marquet, A. *Tetrahedron* **1978,** *34,* 1399. (h) Lett, R.; Chassaing, G.; Marquet, A. *J. Organomet. Chem.* **1976,** *111,* C17. (i) Jordan, T.; Smith, H. W.; Lohr, L. L., Jr.; Lipscomb, W. N. *J. Am. Chem. Soc.* **1963,** *85,* 846. (j) Chassaing, G.; Marquet, A.; Corset, J.; Froment, F. *J. Organomet. Chem.* **1982,** *232,* 293.